

Terephthalate salts: salts of monovalent cations

James A. Kaduk

BP Amoco plc, PO Box 3011, MC F-9,
Naperville, IL 60566, USA

Correspondence e-mail: kadukja@bp.com

The crystal structures of dilithium, disodium and diammonium terephthalate (1,4-benzenedicarboxylate) have been solved *ab initio* using Monte Carlo simulated annealing techniques, and refined using synchrotron powder data. The structures of dipotassium terephthalate, potassium hydrogen terephthalate and ammonium hydrogen terephthalate have been refined using single-crystal techniques. $\text{Li}_2\text{C}_8\text{H}_4\text{O}_4$ crystallizes in $P2_1/c$, with $a = 8.35921(5)$, $b = 5.13208(2)$, $c = 8.48490(5)$ Å, $\beta = 93.1552(4)^\circ$, $V = 363.451(3)$ Å³, $Z = 2$. The Li anions are tetrahedrally coordinated and the packing of the terephthalate anions resembles the γ -packing of aromatic hydrocarbons. $\text{Na}_2\text{C}_8\text{H}_4\text{O}_4$ crystallizes in $Pbc2_1$, with $a = 3.54804(5)$, $b = 10.81604(16)$, $c = 18.99430(20)$ Å, $V = 728.92(2)$ Å³, $Z = 4$. The coordination of the two independent Na is trigonal prismatic and the terephthalate packing resembles the β packing of hydrocarbons. $(\text{NH}_4)_2\text{C}_8\text{H}_4\text{O}_4$ also crystallizes in $Pbc2_1$, with $a = 4.0053(5)$, $b = 11.8136(21)$, $c = 20.1857(24)$ Å, $V = 955.1(2)$ Å³, $Z = 4$. The cations and planar anions are linked by hydrogen bonds and the packing is a looser version of the β packing. $\text{K}_2\text{C}_8\text{H}_4\text{O}_2$ crystallizes in $P2_1/c$, with $a = 10.561(4)$, $b = 3.9440(12)$, $c = 11.535(5)$ Å, $\beta = 113.08(3)^\circ$, $V = 442.0(3)$ Å³, $Z = 2$. The K is trigonal prismatic and the packing is also β . Both $\text{KHC}_8\text{H}_4\text{O}_4$ and $(\text{NH}_4)\text{HC}_8\text{H}_4\text{O}_4$ crystallize in $C2/c$, with $a = 18.825(4)$ and $18.924(4)$, $b = 3.770(2)$ and $3.7967(9)$, $c = 11.179(2)$ and $11.481(2)$ Å, $\beta = 98.04(3)$ and $94.56(5)^\circ$, $V = 816.8(3)$ and $790.9(3)$ Å³, respectively, and $Z = 4$. The packing in the hydrogen-bonded acid salts is also β . Electrostatic interactions among the terephthalate anions appear to be important in determining the crystal packing.

Received 14 July 1999

Accepted 12 November 1999

1. Introduction

Purified terephthalic acid (PTA, 1,4-benzenedicarboxylic acid) is the primary and preferred raw material for the polyester used to make a myriad of consumer and industrial products. BP Amoco technology produces over 3×10^9 Kg of PTA per year. A feed mix of *p*-xylene, catalyst and acetic acid is oxidized with air in a continuous homogeneous reactor, where crude terephthalic acid (TA) is produced (Barker & Saffer, 1958; Partenheimer, 1995). Purified terephthalic acid is then obtained through heterogeneous catalytic hydrogenation and crystallization (Meyer, 1971). From time to time, terephthalate salts are isolated from process streams. Understanding the nature of terephthalate complexes of catalyst and corrosion metals will lead to process insights and improvements.

Very little is known about the solid-state structures of terephthalate salts. Powder diffraction data have been

reported for several metal terephthalates (Sherif, 1970) and the preparations of others have been described (Brzyska, 1971). Only the structures of copper terephthalate dihydrate (Cueto *et al.*, 1991), ammonium hydrogen terephthalate (Cobbledick & Small, 1972), calcium terephthalate trihydrate (Matsuzaki & Itaka, 1977), potassium terephthalate (Ebara & Furuyama, 1973; Furuyama & Ebara, 1967) and potassium hydrogen terephthalate (Miyakubo *et al.*, 1994) have been published.

Most of the terephthalates isolated from commercial operations are intractable solids and consist of mixtures of compounds. We have undertaken a program to prepare pure materials, and understand the solid-state structures of aromatic carboxylates, particularly terephthalates. The classic preparation of terephthalates (Sherif, 1970) involves reaction of TA with base to prepare soluble Na or K terephthalates, which are then reacted with metal salts to yield insoluble terephthalates. These preparations involve excess base, and thus the complexes are prepared at high pH. Since the oxidation of *p*-xylene takes place in acetic acid–water mixtures, it is unclear whether any of these high-pH complexes will be relevant to process chemistry.

In an attempt to prepare a reagent which would permit lower-pH synthesis of terephthalate salts, diammonium terephthalate was prepared. The crystal structure of this compound, as well as those of dilithium and disodium terephthalates, have been determined *ab initio* using X-ray powder diffraction data. Combined with new single-crystal determinations of the structures of dipotassium terephthalate, potassium hydrogen terephthalate and ammonium hydrogen terephthalate, these 'starting materials' begin to give insight into the packing of terephthalate anions in the solid state.

2. Experimental

2.1. Preparation

2.1.1. Dilithium terephthalate. Into 40 ml of distilled water was dissolved 0.3093 g of Li_2O (Pfaltz & Bauer). To this solution was added 1.6712 gm of commercial terephthalic acid. The resulting solution was filtered to remove a few black specks. To this clear solution was added 40 ml ethanol. After evaporating the solvent over two days, a yield of 1.453 gm of white solid was obtained.

2.1.2. Diammonium terephthalate. A quantity of commercial terephthalic acid (9.8100 gm) was placed in an evaporating dish. This dish was placed into a larger container, into which an excess of concentrated aqueous ammonia was poured. The larger container was covered loosely, and the system allowed to equilibrate overnight. The 11.9497 g of white solid produced corresponded to 101% yield of $(\text{NH}_4)_2\text{C}_8\text{H}_4\text{O}_4$.

2.1.3. Disodium terephthalate. Into 5 ml of distilled water was dissolved 1.3792 g of NaOH reagent; the solution was heated on a hot plate. To the clear solution was added 1.7331 g of commercial terephthalic acid. Distilled water was added gradually while heating on the hot plate until all the terephthalic acid was dissolved; approximately 40 ml of water was

required. A small quantity of black solid was removed by filtration. The clear solution was placed back on the hot plate and ethanol was added slowly until a precipitate just began to form at 363 K. A small amount of water was then added to re-dissolve the precipitate. Approximately 30 ml of ethanol was added and the mixture refluxed for ~ 30 min, while a white precipitate formed. The slurry was filtered hot and air-dried. The sodium content of 22% (ICP) corresponded to that expected for $\text{Na}_2\text{C}_8\text{H}_4\text{O}_4$.

2.1.4. Dipotassium terephthalate and potassium hydrogen terephthalate. Into 75 ml of distilled water were dissolved 4.84 g of KOH and 5.00 g of terephthalic acid. The solution was allowed to evaporate and the resulting solid washed several times with methanol to remove excess KOH. The white solid was re-dissolved in distilled water and the solution allowed to evaporate. The resulting solid contained crystals of both dipotassium terephthalate and potassium hydrogen terephthalate.

2.1.5. Ammonium hydrogen terephthalate. To 21.46 g of concentrated aqueous ammonia was added sufficient water to reach a total volume of 40 ml. To this solution was added 3.32 g of terephthalic acid. The mixture was stirred for 1 h, at the end of which it was a white slurry. The slurry was filtered, and the solid was washed with three 20 ml portions of ethanol. Additional solid that formed in the filtrate during the washing was filtered, and combined with the first solid. The combined solid was washed with three 20 ml portions of ethanol. These second washes produced a crystalline solid in the filtrate. The crystal used for data collection was selected from this solid.

2.2. Solution of the structures

2.2.1. Dilithium terephthalate. A laboratory powder pattern (collected on a Scintag PAD V diffractometer equipped with an Ortec intrinsic Ge detector using unfiltered Cu $K\alpha$ radiation) could be indexed (Visser, 1969) on a primitive monoclinic cell having approximate dimensions $a = 8.36$, $b = 5.13$, $c = 8.48$ Å and $\beta = 93.15^\circ$. This cell was also obtained (Boultif & Louer, 1991) from a pattern measured on the X3B1 beamline at the National Synchrotron Light Source at Brookhaven National Laboratory using a wavelength of 1.149681 Å. The pattern was measured from a 1 mm capillary specimen from 2.00 – $56.845^\circ 2\theta$ in 0.005° steps, counting for 4 s per step. The systematic absences determined the space group unambiguously as $P2_1/c$. To obtain a reasonable density, $Z = 2$ and the terephthalate anion occupies a center of symmetry. A planar terephthalate ion was built and minimized using *Cerius*² (Molecular Simulations Inc., 1997), and positioned at the origin. This partial structure was imported into *InsightII* (Molecular Simulations Inc., 1996). The crystal structure was solved using the STRUCTURE_SOLVE module. This module implements a Monte Carlo simulated annealing procedure, in which the metric is not energy, but the agreement of the observed and calculated powder patterns. The 10 – 50° portion of the laboratory pattern was used for the structure solution. Each of the atoms were assigned an occupancy of $\frac{1}{2}$, and the position of the terephthalate was fixed at the origin; only the

Table 1

Fractional atomic coordinates and equivalent isotropic displacement parameters (\AA^2) for $\text{Li}_2(\text{C}_8\text{H}_4\text{O}_4)$.

| | <i>x</i> | <i>y</i> | <i>z</i> | <i>U</i> _{iso} |
|-----|--------------|-------------|-------------|-------------------------|
| C1† | −0.15701 (9) | 0.04934 (5) | 0.04396 (3) | 0.0246 (8) |
| C2† | −0.07238 | −0.16774 | 0.10623 | 0.0246 |
| C3† | 0.08463 | −0.21708 | 0.06227 | 0.0246 |
| H2† | −0.1223 | −0.2834 | 0.17948 | 0.05 |
| H3† | 0.1430 | −0.3668 | 0.10521 | 0.05 |
| C7‡ | −0.3181 (3) | 0.1142 (6) | 0.1018 (4) | 0.0339 (7) |
| O8‡ | −0.3861 (2) | −0.0445 (4) | 0.1902 (3) | 0.0339 |
| O9‡ | −0.3809 (3) | 0.3274 (4) | 0.0532 (3) | 0.0339 |
| Li | 0.4878 (8) | 0.1136 (13) | 0.3556 (8) | 0.0345 (2) |

† Rigid body. ‡ Subject to soft constraints.

orientation of the TA was allowed to vary in the annealing. The procedure quickly converged. This fixed model was used in a Rietveld refinement using *GSAS* (Larson & Von Dreele, 1998) on the synchrotron pattern in which only a scale factor, the background, cell and profile coefficients were refined. A difference Fourier map contained only one significant peak, in a reasonable location for the Li cation.

For the final refinement, the central C_6H_4 portion of the terephthalate was described as a rigid body of half-weight atoms. Soft constraints were applied to the bonded [C1–C7 1.48 (1), C7–O8,O9 1.27 (1) Å] and non-bonded [O8–O9 2.19 (2), C1–O8,O9 2.39 (2), C7–C2,C6 2.51 (2) Å] distances in the carboxyl group. All atoms were refined isotropically. A scale factor and the lattice parameters were refined. Second-order symmetrized spherical harmonic preferred orientation coefficients were refined. The profiles were described by a pseudo-Voigt function (profile function #4). The coefficients *X*, *ptec* (unique axis [100]), *S/L*, *H/L* and the anisotropic strain

broadening tensor terms were refined. The background was described by an eight-term real space pair correlation function.

The final refinement of 44 variables using 9975 observations yielded the residuals $wR_p = 0.0973$, $R_p = 0.0753$, $\chi^2 = 1.973$, $R(F) = 0.1177$ and $R(F^2) = 0.1229$. The soft constraints contributed < 1% of the final χ^2 . Agreement of the observed and calculated patterns (Fig. 1) is excellent. The largest errors are in the description of the profile shapes. The largest peak in a final difference Fourier map was 0.57 e \AA^{-3} (1.84 Å from C7) and the largest difference hole was -0.59 e \AA^{-3} (2.16 Å from Li). A normal probability plot indicated that the standard uncertainties are underestimated by a factor of 1.24. The refined structural parameters are reported in Table 1.

2.2.2. Diammonium terephthalate. The structure of diammonium terephthalate is of interest because I have solved it three times in three different unit cells and three different space groups! The unit cells obtained from laboratory data turned out to be monoclinic subcells of the true orthorhombic cell. (Only the successful refinement is reported here.) The correct cell could be determined only using a synchrotron pattern (Fig. 2). The pattern, measured from 6.00–55.00° 2θ in 0.02° steps on beamline X3B1 at NSLS using a 1 mm quartz capillary specimen and a wavelength of 1.15008 (3) Å, could be indexed on a primitive orthorhombic cell having $a = 4.0053$ (5), $b = 11.8136$ (21), $c = 20.1857$ (24) Å and $V = 955.12$ (23) Å³. The systematic absences were consistent with space groups $Pbc2_1$ or $Pbcm$. To obtain a reasonable density, *Z* must be 4. The natural assumption is that the terephthalate anion occupies a center of symmetry in $Pbcm$ and that the ammonium ion occupies a general position; the cell dimensions correspond to $1 \times 2 \times 2$ terephthalates. All attempts to solve the structure in $Pbcm$ failed; a solution could be obtained only in the true non-centrosymmetric space group $Pbc2_1$.

The structure was also solved using the InsightII STRUC-TURE_SOLV module. A terephthalate anion (including the two carboxyl torsion angles) and two independent ammonium anions were allowed to anneal until a satisfactory minimum was reached. This model served as input to a successful refinement, applying *GSAS* to the laboratory data. (The synchrotron pattern was more difficult to fit, as the anomalous peak shapes, presumably the result of stacking faults, could not be modeled well.)

The C_8H_4 central portion of the terephthalate was treated as a rigid body. The ammonium ions were also described as rigid bodies. Only the positions of the

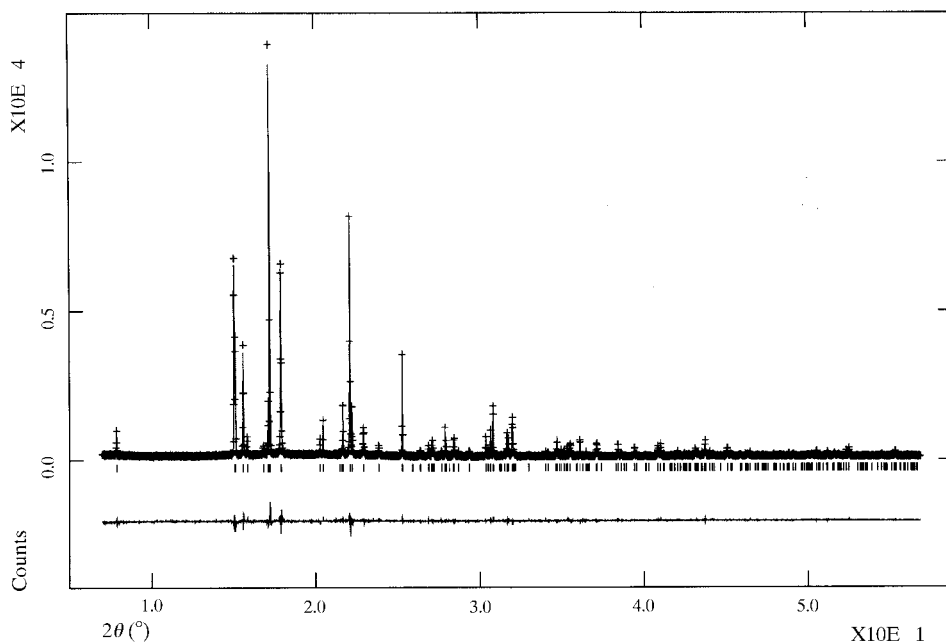


Figure 1

Observed, calculated and difference patterns of $\text{Li}_2(\text{C}_8\text{H}_4\text{O}_4)$. The small crosses represent the observed data points and the solid line through them the calculated pattern. The difference curve is plotted at the same scale as the other patterns. The row of tick marks indicates the positions of the peaks.

Table 2

Fractional atomic coordinates and equivalent isotropic displacement parameters (\AA^2) for $(\text{NH}_4)_2\text{C}_8\text{H}_4\text{O}_4$.

| | <i>x</i> | <i>y</i> | <i>z</i> | <i>U</i> _{iso} |
|-------|------------|--------------|--------------|-------------------------|
| C1† | −0.157 (5) | −0.0853 (11) | 0.0389 (13) | 0.043 (6) |
| C2† | −0.088 | −0.1934 | 0.0152 | 0.043 |
| C3† | −0.171 | −0.2222 | −0.0496 | 0.043 |
| C4† | −0.323 | −0.1429 | −0.0907 | 0.043 |
| C5† | −0.392 | −0.0348 | −0.0670 | 0.043 |
| C6† | −0.309 | −0.0059 | −0.0022 | 0.043 |
| C7† | −0.067 | −0.0541 | 0.1089 | 0.0036 |
| C8† | −0.413 | −0.1740 | −0.1607 | 0.0036 |
| H2† | 0.017 | −0.2481 | 0.0436 | 0.06 |
| H3† | −0.123 | −0.2968 | −0.0659 | 0.06 |
| H5† | −0.497 | 0.0199 | −0.0953 | 0.06 |
| H6† | −0.357 | 0.0686 | 0.0142 | 0.06 |
| O9‡ | −0.070 (5) | −0.1366 (19) | 0.15168 | 0.0036 (3) |
| O10‡ | 0.001 (5) | 0.0464 (17) | 0.1269 (24) | 0.0036 |
| O11‡ | −0.550 (5) | −0.1071 (2) | −0.1998 (8) | 0.0036 |
| O12‡ | −0.483 (5) | −0.2860 (16) | −0.1680 (24) | 0.0036 |
| N13† | 0.504 (4) | 0.1903 (30) | 0.1778 (20) | 0.04 |
| H13a† | 0.445 | 0.2635 | 0.1747 | 0.06 |
| H13b† | 0.329 | 0.1462 | 0.1671 | 0.06 |
| H13c† | 0.674 | 0.1763 | 0.1498 | 0.06 |
| H13d† | 0.569 | 0.1750 | 0.2195 | 0.06 |
| N14† | 0.933 (6) | 0.9226 (25) | 0.2818 (21) | 0.04 |
| H14a† | 1.084 | 0.8666 | 0.2784 | 0.06 |
| H14b† | 0.911 | 0.9428 | 0.3246 | 0.06 |
| H14c† | 1.001 | 0.9827 | 0.2580 | 0.06 |
| H14d† | 0.735 | 0.8983 | 0.2662 | 0.06 |

† Rigid body. ‡ Subject to soft constraints.

ammonium ions were refined; attempts to refine their orientations led to unstable refinements. The hydrogen positions were updated during the course of refinement, by examining the hydrogen-bond geometry around the N atoms and recalculating the hydrogen positions. Soft constraints [C7,C8—O9,O10,O11,O12 1.28 (1), O9···O10, O11···O12

Table 3

Fractional atomic coordinates and equivalent isotropic displacement parameters (\AA^2) for $\text{Na}_2\text{C}_8\text{H}_4\text{O}_4$.

| | <i>x</i> | <i>y</i> | <i>z</i> | <i>U</i> _{iso} |
|-----|------------|--------------|--------------|-------------------------|
| C1† | −0.147 (4) | −0.0979 (19) | −0.0964 (18) | 0.049 (3) |
| C2† | −0.334 | −0.0092 | −0.0548 | 0.049 (3) |
| C3† | −0.434 | −0.0373 | 0.0152 | 0.049 (3) |
| C4† | −0.346 | −0.1541 | 0.0437 | 0.049 (3) |
| C5† | −0.159 | −0.2429 | 0.0021 | 0.049 (3) |
| C6† | −0.059 | −0.2148 | −0.0679 | 0.049 (3) |
| H2† | −0.394 | 0.0714 | −0.0744 | 0.04 |
| H3† | −0.563 | 0.0239 | 0.0439 | 0.04 |
| H5† | −0.098 | −0.3235 | 0.0217 | 0.04 |
| H6† | 0.070 | −0.276 | −0.0966 | 0.04 |
| C7‡ | −0.058 (7) | −0.0783 (19) | −0.1727 (18) | 0.0187 (15) |
| C8‡ | −0.419 (7) | −0.1745 (22) | 0.1208 (17) | 0.0187 |
| O1‡ | −0.024 (4) | 0.0322 (21) | −0.1976 (19) | 0.0187 |
| O2‡ | −0.038 (4) | −0.1677 (23) | −0.2133 (19) | 0.0187 |
| O3‡ | −0.484 (4) | −0.2860 (23) | 0.1426 (19) | 0.0187 |
| O4‡ | −0.503 (5) | −0.0826 (24) | 0.1574 (18) | 0.0187 |
| Na1 | −1.014 (4) | 0.5712 (31) | 0.17715 (3) | 0.0226 (13) |
| Na2 | 0.479 (2) | 0.3194 (31) | 0.27253 | 0.0226 |

† Rigid body. ‡ Subject to soft constraints.

2.22 (2), C1,C4···O9,O10,O11,O12 2.42 (2) \AA] were applied to the bonded and non-bonded distances involving the carboxylate O atoms. The origin was defined by fixing the *z* coordinate of O9. All atoms were refined isotropically. A scale factor and the lattice parameters were refined. A March–Dollase preferred orientation *ratio* (unique axis = [001]) was refined. The peak profiles were described by a pseudo-Voigt function (profile function #2). Only the strain broadening terms *Y* and *stec* [unique axis = (001)] refined to values different than those of the instrumental profile function. A sample displacement coefficient was refined. The background was described by an eight-term real space pair correlation function, with fixed characteristic distances of 0.70, 4.40 and 8.00 \AA .

The final refinement of 38 variables using 3108 observations yielded the residuals $wR_p = 0.1790$, $R_p = 0.1335$, $\chi^2 = 7.365$, $R(F) = 0.0724$, $R(F^2) = 0.1339$. The soft constraints contributed < 1% of the final χ^2 . Agreement of the observed and calculated patterns (Fig. 3) is acceptable. The residuals indicate that this material is afflicted with stacking faults, which have not been analyzed completely. The quality of the refinement indicates the limits to which a crystalline model can be forced to this more-complex structure. The largest peak in a final difference Fourier map was 0.40 e \AA^{-3} (0.72 \AA from O12), and the largest difference hole was -0.35 e \AA^{-3} (1.22 \AA from H14a). A normal probability plot indicated

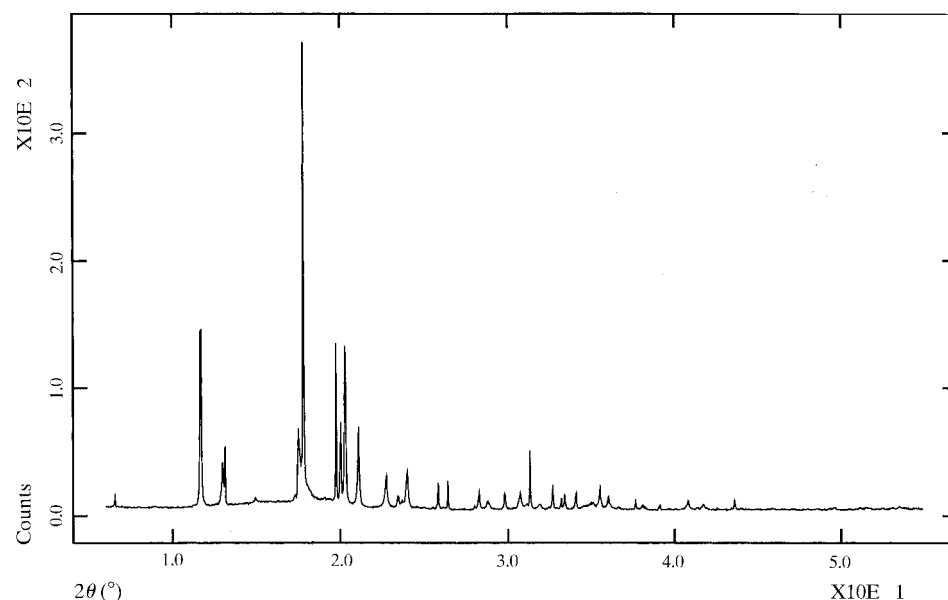


Figure 2

Synchrotron powder pattern of $(\text{NH}_4)_2\text{C}_8\text{H}_4\text{O}_4$.

Table 4

Experimental details.

| | K ₂ TA | KHTA | NH ₄ HTA |
|--|--|--|--|
| Crystal data | | | |
| Chemical formula | 2K ⁺ .C ₈ H ₄ O ₄ ²⁻ | K ⁺ .C ₈ H ₅ O ₄ ⁻ | (NH ₄) ⁺ .C ₈ H ₅ O ₄ ⁻ |
| Chemical formula weight | 242.31 | 204.22 | 183.16 |
| Cell setting | Monoclinic | Monoclinic | Monoclinic |
| Space group | <i>P</i> 2 ₁ / <i>c</i> | <i>C</i> ₂ / <i>c</i> | <i>C</i> ₂ / <i>c</i> |
| <i>a</i> (Å) | 10.561 (4) | 18.825 (4) | 18.924 (4) |
| <i>b</i> (Å) | 3.9440 (12) | 3.7700 (8) | 3.7967 (8) |
| <i>c</i> (Å) | 11.535 (5) | 11.179 (2) | 11.481 (2) |
| β (°) | 113.08 (3) | 94.56 (3) | 98.04 (3) |
| <i>V</i> (Å ³) | 442.0 (3) | 790.9 (3) | 816.8 (3) |
| <i>Z</i> | 2 | 4 | 4 |
| <i>D_x</i> (Mg m ⁻³) | 1.821 | 1.715 | 1.489 |
| Radiation type | Mo <i>K</i> α | Mo <i>K</i> α | Mo <i>K</i> α |
| Wavelength (Å) | 0.71073 | 0.71073 | 0.71073 |
| No. of reflections for cell parameters | 19 | 7 | 10 |
| θ range (°) | 5.51–11.36 | 2.00–20.00 | 2.00–20.00 |
| μ (mm ⁻¹) | 1.052 | 0.645 | 0.121 |
| Temperature (K) | 294 | 298 | 298 |
| Crystal form | Needle | Plate | Plate |
| Crystal size (mm) | 0.45 × 0.05 × 0.05 | 0.42 × 0.10 × 0.04 | 0.3 × 0.2 × 0.05 |
| Crystal color | Colorless | Colorless | Colorless |
| Data collection | | | |
| Diffractometer | Scintillation counter | Scintillation counter | Scintillation counter |
| Data collection method | θ –2 θ scans | θ –2 θ scans | θ –2 θ scans |
| Absorption correction | None | None | None |
| No. of measured reflections | 1130 | 695 | 785 |
| No. of independent reflections | 584 | 376 | 373 |
| No. of observed reflections | 497 | 296 | 307 |
| Criterion for observed reflections | <i>I</i> > 2 σ (<i>I</i>) | <i>I</i> > 2 σ (<i>I</i>) | <i>I</i> > 2 σ (<i>I</i>) |
| <i>R</i> _{int} | 0.0228 | 0.0287 | 0.0187 |
| θ _{max} (°) | 22.54 | 20.04 | 20.01 |
| Range of <i>h</i> , <i>k</i> , <i>l</i> | 0 → <i>h</i> → 11 –4 → <i>k</i> → 4 –12 → <i>l</i> → 11 | 0 → <i>h</i> → 18 –3 → <i>k</i> → 3 –10 → <i>l</i> → 10 | –18 → <i>h</i> → 18 –3 → <i>k</i> → 3 –11 → <i>l</i> → 11 |
| No. of standard reflections | 5 | 5 | 6 |
| Frequency of standard reflections | Every 200 reflections | Every 200 reflections | Every 200 reflections |
| Refinement | | | |
| Refinement on | <i>F</i> ² | <i>F</i> ² | <i>F</i> ² |
| <i>R</i> [<i>F</i> ² > 2 σ (<i>F</i> ²)] | 0.0248 | 0.0302 | 0.0293 |
| <i>wR</i> (<i>F</i> ²) | 0.0607 | 0.0715 | 0.0755 |
| <i>S</i> | 1.074 | 1.018 | 0.995 |
| No. of reflections used in refinement | 584 | 376 | 373 |
| No. of parameters used | 66 | 72 | 80 |
| H-atom treatment | Mixed | Mixed | Mixed |
| Weighting scheme | $w = 1/[\sigma^2(F_o^2) + (0.0339P)^2 + 0.0595P]$, where $P = (F_o^2 + 2F_c^2)/3$ | $w = 1/[\sigma^2(F_o^2) + (0.0438P)^2]$, where $P = (F_o^2 + 2F_c^2)/3$ | $w = 1/[\sigma^2(F_o^2) + (0.0536P)^2]$, where $P = (F_o^2 + 2F_c^2)/3$ |
| (Δ/σ) _{max} | 0.010 | 0.017 | 0.243 |
| $\Delta\rho$ _{max} (e Å ⁻³) | 0.216 | 0.145 | 0.106 |
| $\Delta\rho$ _{min} (e Å ⁻³) | –0.194 | –0.153 | –0.178 |
| Extinction method | None | None | None |
| Source of atomic scattering factors | <i>International Tables for Crystallography</i> (1992, Vol. C, Tables 4.2.6.8 and 6.1.1.4) | <i>International Tables for Crystallography</i> (1992, Vol. C, Tables 4.2.6.8 and 6.1.1.4) | <i>International Tables for Crystallography</i> (1992, Vol. C, Tables 4.2.6.8 and 6.1.1.4) |
| Computer programs | | | |
| Data collection | <i>P3</i> (Nicolet, 1988) | <i>P3</i> (Nicolet, 1988) | <i>P3</i> (Nicolet, 1988) |
| Cell refinement | <i>P3</i> (Nicolet, 1988) | <i>P3</i> (Nicolet, 1988) | <i>P3</i> (Nicolet, 1988) |
| Data reduction | <i>XTAPE</i> (Nicolet, 1988) | <i>XTAPE</i> (Nicolet, 1988) | <i>XTAPE</i> (Nicolet, 1988) |
| Structure solution | <i>SHELXS97</i> (Sheldrick, 1990) | <i>SHELXS97</i> (Sheldrick, 1990) | <i>SHELXS97</i> (Sheldrick, 1990) |
| Structure refinement | <i>SHELXL97</i> (Sheldrick, 1997) | <i>SHELXL97</i> (Sheldrick, 1997) | <i>SHELXL97</i> (Sheldrick, 1997) |

that the standard uncertainties are underestimated by a factor of 2.25. The refined structural parameters are reported in Table 2.

2.2.3. Disodium terephthalate. The powder pattern was measured from a 1 mm capillary specimen at beamline X3B1 at NSLS, using a wavelength of 1.149681 Å. The pattern was

measured from 3.000 to 55.330° in 0.005° steps, counting for 4 s per step. The pattern could be indexed (Boultif & Louer, 1991) on a primitive orthorhombic unit cell having $a = 3.54788$ (8), $b = 10.8167$ (2), $c = 18.995$ (4) Å. The similarity of the cell to that of diammonium terephthalate suggested that there might be some relation between the structures. Accordingly, a terephthalate anion (including the two

carboxyl torsion angles) and two sodium cations were used as input to simulated annealing runs in space group $Pbc2_1$ using STRUCTURE_SOLVE. The best arrangement of anions was very similar to that in diammonium terephthalate, but one of the sodium cation positions was chemically unreasonable. The positions of the terephthalate atoms were fixed and a symmetry-constrained molecular mechanics minimization of

the crystal structure was carried out using Cerius² (Universal force field). The two sodium cations moved to positions from which a successful Rietveld refinement could be obtained.

The 6.000 – 55.000° 2θ portion of the pattern was included in the refinement. The central C_6H_4 portion of the terephthalate was treated as a rigid body; the single translation used to define the body was refined to a value of 1.409 (3) Å. Soft constraints were applied to the bonded [C1,C4–C7,C8 1.50 (1), C7,C8–O1,O2,-O3,O4 1.28 (1) Å] and non-bonded [O1–O2,O3–O4 2.21 (2), C1,C4–O1,O2,O3,O4 2.41 (2), C7,C8–C2,C6,C3,C5 2.51 (2) Å] distances involving the carboxyl groups. The origin was defined by fixing the z coordinate of Na2. All atoms were refined isotropically; the displacement coefficients of the ring C atoms, the atoms of the carboxyl groups and the two Na were constrained to have the same values.

Scale factors for both disodium terephthalate and a trona, $Na_3H(CO_3)_2(H_2O)_2$, impurity were refined. (Disodium terephthalate reacts slowly with atmospheric CO_2 .) The lattice parameters of both phases were refined. The peak profiles were described by a pseudo-Voigt function (profile function #2). Only the size broadening terms X and $ptec$ (unique axis [001]) and the strain broadening term Y refined to values different than those of the instrumental profile function. The background was described by a six-term cosine Fourier series.

The final refinement of 53 variables using 9815 observations yielded the residuals $wR_p = 0.1980$, $R_p = 0.1473$, $\chi^2 = 6.623$, $R(F) =$

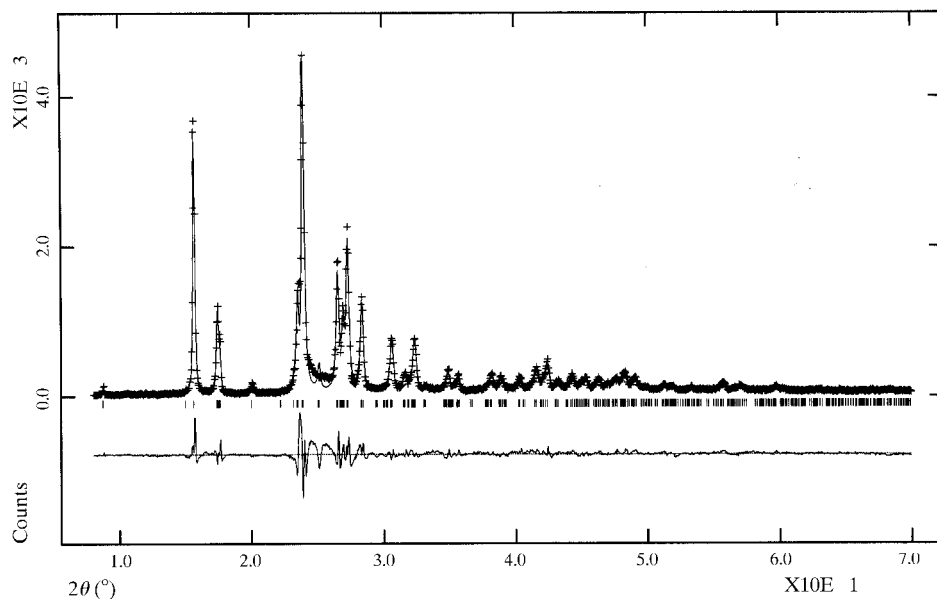


Figure 3

Observed, calculated and difference patterns of $(NH_4)_2(C_8H_4O_4)$. The small crosses represent the observed data points and the solid line through them the calculated pattern. The difference curve is plotted at the same scale as the other patterns. The row of tick marks indicates the positions of the peaks.

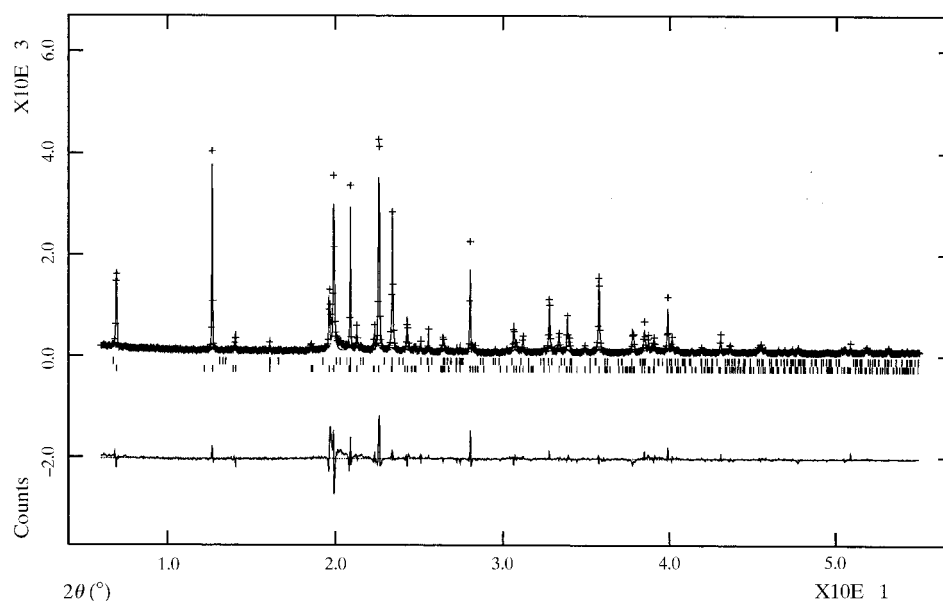


Figure 4

Observed, calculated and difference patterns of $Na_2C_8H_4O_4$. The small crosses represent the observed data points and the solid line through them the calculated pattern. The difference curve is plotted at the same scale as the other patterns. The bottom row of tick marks indicates the positions of the disodium terephthalate peaks and the top row marks the positions of the peaks of the trona, $Na_3H(CO_3)_2(H_2O)_2$, impurity.

Table 5

Fractional atomic coordinates and equivalent isotropic displacement parameters (\AA^2) for $\text{K}_2\text{C}_8\text{H}_4\text{O}_4$.

| | $U_{\text{eq}} = (1/3)\Sigma_i \Sigma_j U^{ij} a^i a^j \mathbf{a}_i \cdot \mathbf{a}_j$ | | | |
|-----|---|--------------|---------------|-----------------|
| | <i>x</i> | <i>y</i> | <i>z</i> | U_{eq} |
| K1 | 0.61068 (6) | 0.20395 (14) | 0.16167 (5) | 0.0268 (2) |
| O1 | 0.35218 (18) | 0.1856 (5) | 0.16464 (16) | 0.0290 (5) |
| O2 | 0.32648 (19) | 0.3005 (5) | −0.03264 (17) | 0.0291 (5) |
| C7 | 0.2822 (3) | 0.2858 (6) | 0.0541 (2) | 0.0207 (6) |
| C1 | 0.1358 (3) | 0.3988 (6) | 0.0259 (2) | 0.0214 (6) |
| C2 | 0.0787 (3) | 0.3548 (7) | 0.1146 (2) | 0.0244 (7) |
| C6 | 0.0548 (3) | 0.5466 (7) | −0.0895 (2) | 0.0255 (7) |
| H2A | 0.1312 | 0.2575 | 0.1921 | 0.027 (7) |
| H6A | 0.0913 | 0.5789 | −0.1502 | 0.029 (7) |

0.1039, $R(F^2) = 0.1472$. The soft constraints contributed 0.8% of the final χ^2 . The agreement of the observed and calculated patterns (Fig. 4) makes it clear that the profiles were not described completely and that this material suffers from stacking faults; the structure reported here is thus an average structure. The largest peak in a final difference map was 0.48 e \AA^{-3} , 0.75 \AA from Na2, and the largest difference hole was -0.41 e \AA^{-3} , 1.79 \AA from H6. A normal probability plot indicated that the standard uncertainties were underestimated by a factor of 1.9. The refined structural parameters are reported in Table 3.

2.2.4. Dipotassium, potassium hydrogen and ammonium hydrogen terephthalates. Single crystal data sets on small crystals of these three compounds were collected on a Nicolet R3m/V system equipped with a scintillation detector and graphite monochromator, using Mo $K\alpha$ radiation. Data collection and refinement are summarized in Table 4. The structures were solved using direct methods (Sheldrick, 1997). The fractional atomic coordinates and isotropic displacement coefficients are reported in Tables 5–7, and the anisotropic displacement coefficients are listed in Tables 8–10. The calculated powder patterns of all six compounds have been submitted to the International Centre for Diffraction Data for inclusion in the Powder Diffraction File.¹

3. Results

The bond distances and angles in the carboxyl groups of the terephthalate anions are reported in Table 11. The C–O bonds in dilithium and dipotassium terephthalate are equivalent, and these bonds appear to be resonant. The C–O bond lengths in diammonium and disodium terephthalate differ and the bonds may exhibit partial single/double bond character. In the two acid salts, one C–O bond is short and corresponds to a carbonyl group, while the other is intermediate in length between a single and double bond; this bond is to the oxygen participating in hydrogen bonds. The C–C–O and O–C–O angles fall within the normal ranges (Kaduk & Golab, 1999). The distances and angles obtained from the

¹Supplementary data for this paper are available from the IUCr electronic archives (Reference: BK0069). Services for accessing these data are described at the back of the journal.

Table 6

Fractional atomic coordinates and equivalent isotropic displacement parameters (\AA^2) for $\text{KHC}_8\text{H}_4\text{O}_4$.

| | $U_{\text{eq}} = (1/3)\Sigma_i \Sigma_j U^{ij} a^i a^j \mathbf{a}_i \cdot \mathbf{a}_j$ | | | |
|-----|---|-------------|------------|-----------------|
| | <i>x</i> | <i>y</i> | <i>z</i> | U_{eq} |
| K | 0 | 0.3441 (4) | 1/4 | 0.0458 (6) |
| O1 | 0.08687 (11) | 0.1788 (8) | 0.6571 (2) | 0.0346 (8) |
| O2 | 0.06011 (13) | 0.0413 (9) | 0.4658 (2) | 0.0447 (9) |
| C4 | 0.10416 (17) | 0.1391 (11) | 0.5544 (4) | 0.0248 (10) |
| C1 | 0.17938 (16) | 0.1986 (10) | 0.5236 (3) | 0.0221 (10) |
| C2 | 0.20168 (19) | 0.1064 (11) | 0.4125 (4) | 0.0239 (10) |
| C6 | 0.22783 (18) | 0.3424 (12) | 0.6104 (4) | 0.0251 (10) |
| H1† | 0.0168 (17) | 0.08 (2) | 0.477 (7) | 0.04 (3) |
| H2 | 0.1735 (17) | 0.013 (9) | 0.349 (3) | 0.011 (9) |
| H6 | 0.2123 (17) | 0.403 (9) | 0.683 (3) | 0.026 (10) |

† Occupancy = $\frac{1}{2}$, subject to soft constraint.

Table 7

Fractional atomic coordinates and equivalent isotropic displacement parameters (\AA^2) for $(\text{NH}_4)_2\text{HC}_8\text{H}_4\text{O}_4$.

| | $U_{\text{eq}} = (1/3)\Sigma_i \Sigma_j U^{ij} a^i a^j \mathbf{a}_i \cdot \mathbf{a}_j$ | | | |
|-----|---|-------------|--------------|-----------------|
| | <i>x</i> | <i>y</i> | <i>z</i> | U_{eq} |
| O1 | 0.09478 (9) | 0.1447 (5) | 0.65460 (15) | 0.0429 (7) |
| O2 | 0.05923 (10) | 0.0337 (6) | 0.46591 (16) | 0.0454 (7) |
| C4 | 0.10757 (14) | 0.1194 (7) | 0.5524 (2) | 0.0307 (8) |
| C1 | 0.18055 (13) | 0.1862 (6) | 0.5232 (2) | 0.0246 (8) |
| C2 | 0.19949 (14) | 0.1088 (7) | 0.4134 (2) | 0.0287 (8) |
| C6 | 0.23173 (14) | 0.3281 (7) | 0.6095 (2) | 0.0295 (8) |
| H2A | 0.1644 (13) | 0.004 (6) | 0.354 (2) | 0.031 (7) |
| H6A | 0.2178 (12) | 0.383 (7) | 0.685 (2) | 0.037 (7) |
| N1 | 1/2 | 0.0908 (14) | 3/4 | 0.0459 (10) |
| H1 | 0.5335 (19) | −0.046 (10) | 0.721 (3) | 0.080 (12) |
| H2 | 0.475 (2) | 0.189 (12) | 0.688 (4) | 0.106 (17) |
| H3† | 0.021 (2) | 0.00 (2) | 0.496 (6) | 0.050 (18) |

† Occupancy = $\frac{1}{2}$, subject to soft constraint.

Rietveld refinements are comparable to those obtained from single-crystal data.

None of the terephthalate anions are completely planar. In four of them, the carboxyl groups are rotated only slightly out of the ring plane ($6\text{--}10^\circ$), but in diammonium and disodium terephthalate the deviation from planarity is significant ($21\text{--}31^\circ$). Even these large rotations result in only a small energy penalty ($8\text{--}19 \text{ kJ mol}^{-1}$; Kaduk & Golab, 1999). Aromatic carboxylates are more flexible than is commonly believed. These rotations result in more favorable coordination geometries.

One of the Li–O bonds in dilithium terephthalate is short (Li–O9 1.906 \AA), while the other three (Li–O9 1.976 , Li–O8 1.975 , 1.979 \AA) are similar. The average bond distance in a LiO_4 coordination sphere in the Cambridge Structural Database (Allen & Kennard, 1993) is $1.96 (9) \text{ \AA}$; these distances are therefore typical. The Li atomic valence, calculated from the sum of bond valences (Bresle & O'Keefe, 1991), is 1.06. The Li coordination is tetrahedral; the average deviation of the O–Li–O angles from the ideal tetrahedral value is 8.9° . Each oxygen is coordinated to two different Li. There is no chelation; the carboxyl groups bridge lithium cations.

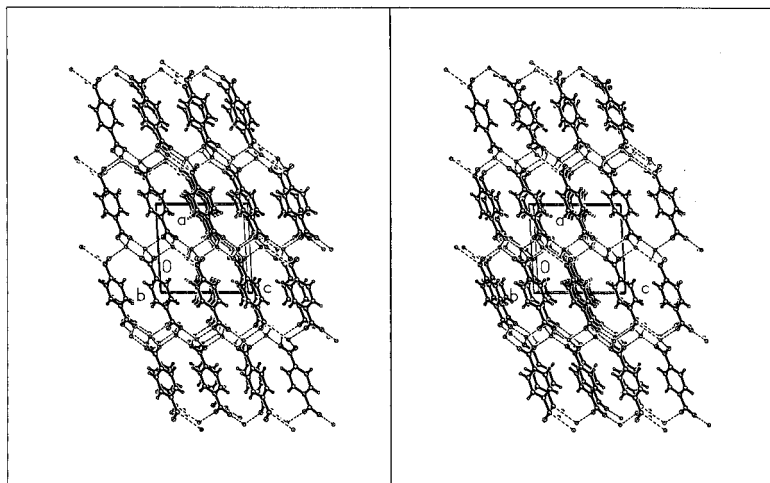


Figure 5
A stereo illustration of the crystal structure of $\text{Li}_2\text{C}_8\text{H}_4\text{O}_4$. The view is down the monoclinic b axis.

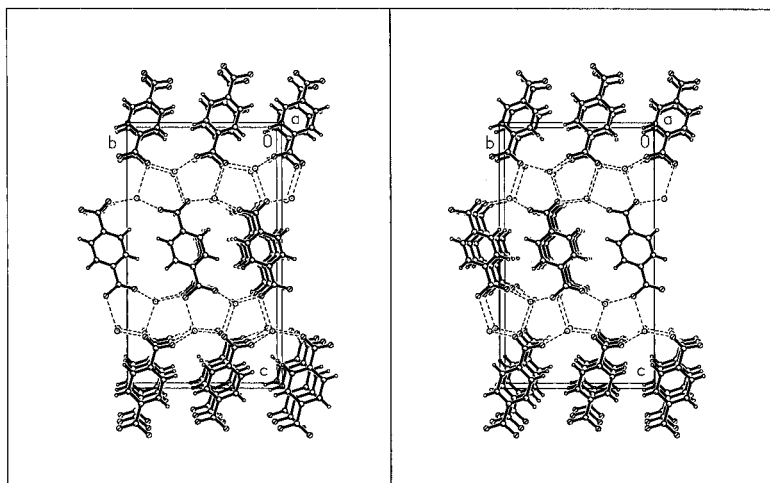


Figure 6
A stereo view of the crystal structure of $(\text{NH}_4)_2\text{C}_8\text{H}_4\text{O}_4$. The view is down the orthorhombic a axis. The H atoms of the ammonium cations have been omitted for clarity. Potential $\text{N}-\text{H}\cdots\text{O}$ hydrogen bonds are indicated by dashed lines.

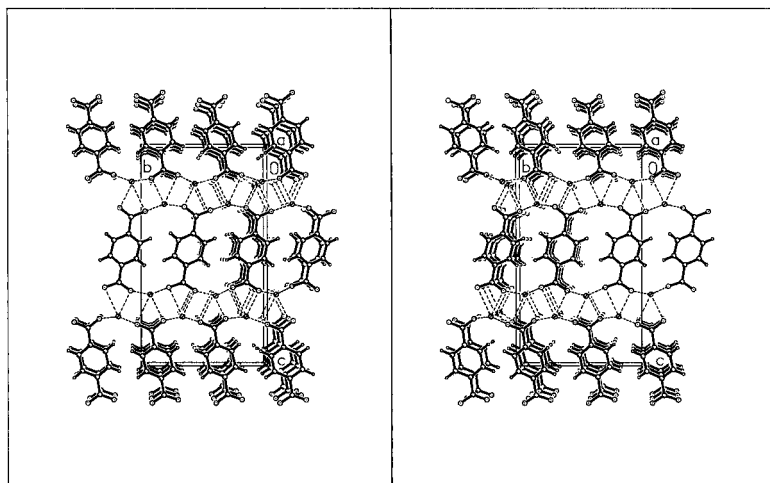


Figure 7
A stereo view of the crystal structure of $\text{Na}_2\text{C}_8\text{H}_4\text{O}_4$. The view is down the orthorhombic a axis.

In diammonium terephthalate, each nitrogen is surrounded by four O atoms ($\text{N13}-\text{O}$ 2.66–2.83, $\text{N14}-\text{O}$ 2.53–3.02 Å) in an approximately tetrahedral arrangement. Each oxygen can be hydrogen-bonded to potentially two N atoms. The $\text{N}\cdots\text{O}$ distances indicate that some of these hydrogen bonds are strong (Jeffrey, 1997). Molecular mechanics calculations (*Cerius²* COMPASS force field, fixed heavy atom positions) indicate that crystal energy depends only slightly on the orientations of the ammonium ions. The displacement coefficients of the atoms of the carboxyl groups are apparently much lower than those of the other atoms in these compounds. This low value probably reflects the faulting in this structure; we have observed similar low values for carboxylates in other defective structures (Kaduk & Golab, 1999).

The Na–O bond distances in disodium terephthalate span a wide range ($\text{Na1}-\text{O}$ 2.33, 2.37, 2.42, 2.50, 2.52, 2.63 Å, $\text{Na2}-\text{O}$ 2.28, 2.43, 2.45, 2.47, 2.59, 2.72 Å). The average distance in an NaO_6 coordination sphere in the CSD is 2.43 (12) Å. The Na atomic valences, calculated from the sums of bond valences, are 1.04 and 0.99. The coordination of each Na is trigonal prismatic. Each carboxyl group chelates to one Na and is coordinated to four others, two each above and below the chelation plane. The chelation is asymmetric; $\text{Na1}-\text{O1}$ 2.63, $\text{Na1}-\text{O2}$ 2.33 Å and $\text{Na2}-\text{O3}$ 2.72, $\text{Na2}-\text{O4}$ 2.43 Å. Each oxygen is coordinated to three different Na.

The potassium coordination in dipotassium terephthalate is similar to that in the disodium salt. The K coordination is trigonal prismatic and the K–O distances (2.68, 2.69, 2.72, 2.74, 2.78, 2.98) agree well with the 2.79 (16) Å expected in a KO_6 coordination sphere in the CSD. The K atomic valence, calculated from the sums of bond valences, is 1.11.

In potassium hydrogen terephthalate, the K coordination is distorted octahedral ($\text{K}-\text{O}$ 2.70 × 2, 2.81 × 2, 2.82 × 2 Å). The average deviation from the ideal octahedral angles is 13°. The carbonyl oxygen O1 is coordinated to two different K, while O2 is bonded to one K and participates in a very strong hydrogen bond ($\text{O2}\cdots\text{O2}$ 2.46 Å). There is a center of symmetry midway between the two O2 in the hydrogen bond. As found by Miyakubo *et al.* (1994), a significantly better refinement was obtained by displacing the hydrogen from the center of symmetry. It would be very difficult to distinguish a single-minimum from a double-minimum hydrogen bond using room-temperature X-ray data from such a small crystal.

The $\text{N}\cdots\text{O}$ distances in ammonium hydrogen terephthalate (2.80 × 2 and 2.94 × 2 Å, with two more at 3.07 Å) are appropriate for hydrogen bonding. As in potassium hydrogen terephthalate,

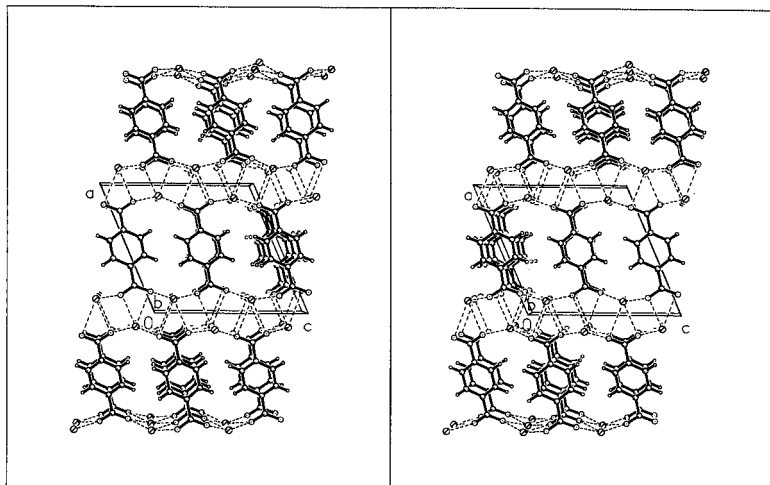


Figure 8
A stereo view of the crystal structure of $K_2C_8H_4O_4$. The view is down the monoclinic b axis.

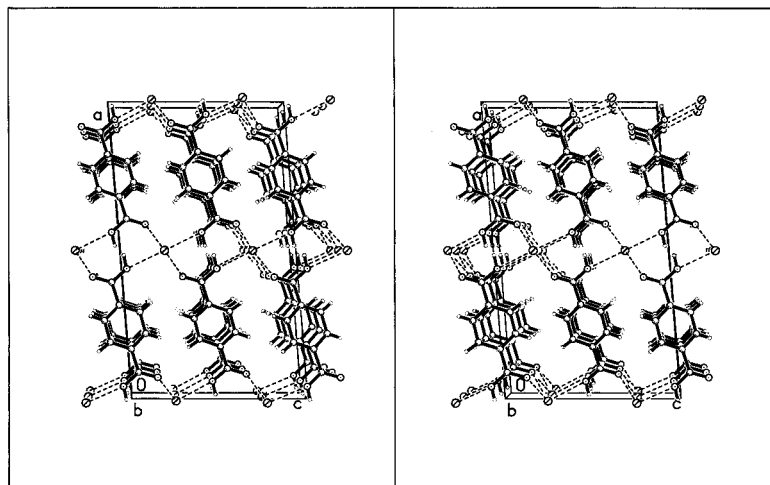


Figure 9
A stereo view of the crystal structure of $KHC_8H_4O_4$. The view is down the monoclinic b axis.

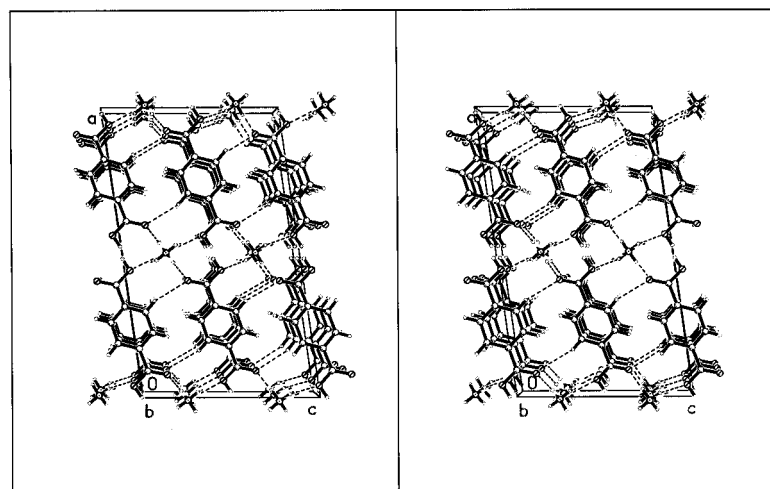


Figure 10
A stereo view of the crystal structure of $(NH_4)HC_8H_4O_4$. The view is down the monoclinic b axis.

O2 participates in a very strong hydrogen bond ($O2 \cdots O2$ 2.49 Å). Cobblecick & Small (1972) described the hydrogen bond as symmetric, but a significantly better refinement was obtained here by allowing the hydrogen to move off the center of symmetry.

4. Discussion

As might be expected, these crystal structures (Figs. 5–10) consist of alternating layers of aromatic rings and cations/O atoms ('hydrophobic' and 'hydrophilic'). Perhaps surprisingly, the packings of the terephthalate anions follow patterns established for aromatic hydrocarbons (Desiraju & Gavezzotti, 1989*a,b*; Gavezzotti & Desiraju, 1988). Four characteristic packings of these flat molecules have been identified: herringbone (HB), stacked herringbone (SHB), γ and β . The key parameters separating the four structure types are the shortest cell axis and the interplanar angle, defined as the angle between the mean plane of one molecule and that of its nearest neighbors.

For hydrocarbons with short axes less than ~ 4 Å, β -structures with small interplanar angles are observed (Fig. 11). The region between short axes 4.1 and 4.6 Å is apparently forbidden for planar aromatics. The γ -structures cluster in the axial range 4.6–5.4 Å, while the HB and SHB structures are observed for larger axial lengths. The crucial link between molecular and crystal structure is the relative ability of a molecule to employ $C \cdots C$, $C \cdots H$ and $H \cdots H$ interactions. Stacking, in which $C \cdots C$ interactions are important, is prominent in both γ - and β -structures. $C \cdots H$ interactions are more prominent in γ -structures than in β -structures.

The terephthalate packing in the dilithium salt is γ (Fig. 12), consistent with the short axis of 5.13208(2) Å and the interplanar angle of 67.8°. The other five compounds in this study exhibit the β packing (Fig. 13); the short axes and interplanar angles are listed in Table 12. The fact that the short axes and packings fall into the pattern of aromatic hydrocarbons indicates that aromatic–aromatic interactions play an important role in determining these crystal structures. The interplanar angles, however, differ from those observed in hydrocarbon packings, demonstrating that cation–anion interactions are also important.

The stacking of the parallel terephthalates in the β -structures (Fig. 14) results in short $C \cdots C$ distances (as short as 3.15 Å in disodium terephthalate and 3.47 Å in the other salts) between neighboring benzene rings, but maximizes attractive interactions between partially negative carboxyl O atoms and partially positive carboxyl C

Table 8
Anisotropic displacement parameters (\AA^2) for dipotassium terephthalate.

| | U^{11} | U^{22} | U^{33} | U^{12} | U^{13} | U^{23} |
|----|-------------|-------------|-------------|--------------|-------------|--------------|
| K1 | 0.0284 (4) | 0.0280 (4) | 0.0273 (4) | 0.0002 (3) | 0.0146 (3) | -0.0010 (3) |
| O1 | 0.0230 (10) | 0.0399 (12) | 0.0230 (11) | 0.0045 (9) | 0.0078 (9) | 0.0071 (9) |
| O2 | 0.0274 (10) | 0.0368 (12) | 0.0292 (10) | 0.0055 (9) | 0.0176 (9) | 0.0009 (9) |
| C7 | 0.0213 (14) | 0.0176 (14) | 0.0253 (15) | -0.0013 (11) | 0.0114 (13) | -0.0028 (11) |
| C1 | 0.0226 (14) | 0.0210 (14) | 0.0215 (14) | -0.0025 (12) | 0.0097 (12) | -0.0023 (11) |
| C2 | 0.0219 (15) | 0.0309 (16) | 0.0195 (14) | 0.0041 (12) | 0.0071 (12) | 0.0050 (11) |
| C6 | 0.0272 (16) | 0.0321 (16) | 0.0218 (14) | 0.0002 (13) | 0.0146 (12) | 0.0021 (12) |

Table 9
Anisotropic displacement parameters (\AA^2) for potassium hydrogen terephthalate.

| | U^{11} | U^{22} | U^{33} | U^{12} | U^{13} | U^{23} |
|----|-------------|------------|-------------|--------------|--------------|--------------|
| K | 0.0524 (9) | 0.0419 (9) | 0.0465 (9) | 0.000 | 0.0251 (7) | 0.000 |
| O1 | 0.0234 (15) | 0.055 (2) | 0.0270 (16) | -0.0062 (15) | 0.0102 (12) | -0.0048 (15) |
| O2 | 0.0135 (16) | 0.087 (3) | 0.0332 (17) | -0.0107 (16) | 0.0024 (15) | -0.0042 (17) |
| C4 | 0.016 (2) | 0.027 (2) | 0.032 (3) | -0.004 (2) | 0.001 (2) | 0.001 (2) |
| C1 | 0.014 (2) | 0.021 (2) | 0.030 (3) | -0.0034 (19) | -0.005 (2) | 0.0007 (19) |
| C2 | 0.021 (2) | 0.030 (3) | 0.020 (2) | -0.005 (2) | -0.0006 (19) | -0.004 (2) |
| C6 | 0.024 (2) | 0.031 (2) | 0.022 (2) | 0.003 (2) | 0.010 (2) | 0.005 (2) |

Table 10
Anisotropic displacement parameters (\AA^2) for ammonium hydrogen terephthalate.

| | U^{11} | U^{22} | U^{33} | U^{12} | U^{13} | U^{23} |
|----|-------------|-------------|-------------|--------------|--------------|--------------|
| O1 | 0.0298 (12) | 0.0699 (15) | 0.0310 (12) | -0.0041 (10) | 0.0114 (8) | -0.0016 (10) |
| O2 | 0.0209 (12) | 0.0811 (16) | 0.0341 (12) | -0.0141 (13) | 0.0034 (10) | 0.0001 (11) |
| C4 | 0.0244 (19) | 0.0352 (17) | 0.0324 (17) | -0.0015 (13) | 0.0038 (15) | 0.0018 (14) |
| C1 | 0.0197 (17) | 0.0289 (15) | 0.0250 (15) | -0.0020 (13) | 0.0024 (15) | 0.0006 (13) |
| C2 | 0.0219 (18) | 0.0352 (16) | 0.0276 (15) | -0.0046 (14) | -0.0015 (14) | -0.0031 (14) |
| C6 | 0.029 (2) | 0.0373 (18) | 0.0231 (16) | 0.0007 (14) | 0.0065 (15) | 0.0002 (14) |
| N1 | 0.049 (3) | 0.050 (3) | 0.042 (3) | 0.000 | 0.020 (3) | 0.000 |

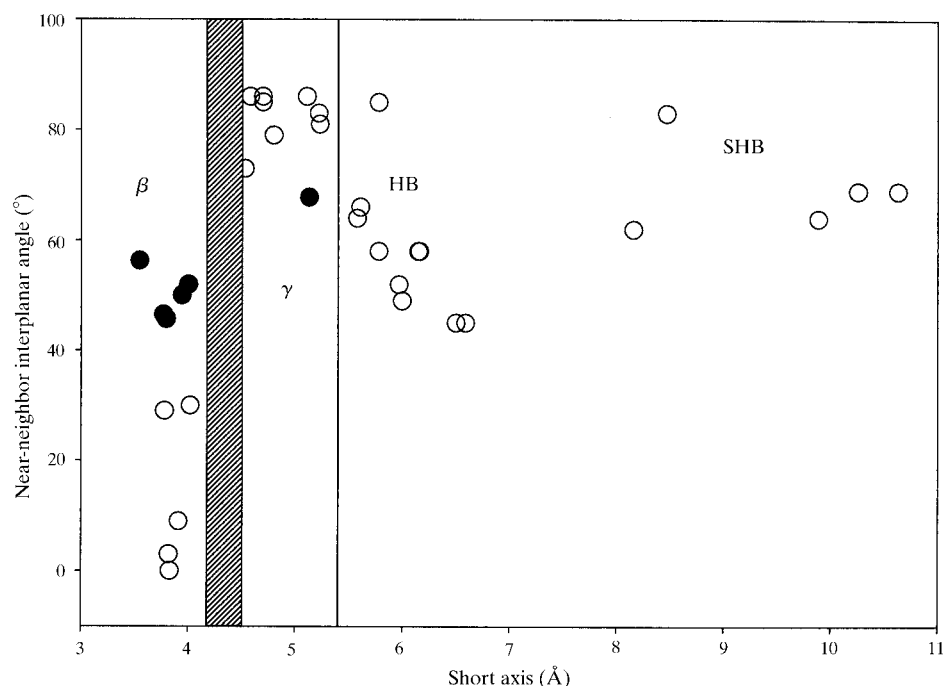


Figure 11
Intermolecular interplanar angle versus the shortest cell axis. The open circles represent the aromatic hydrocarbons of Desiraju & Gavezzotti (1989a) and the filled circles the terephthalate salts of this work.

atoms, and minimizes the repulsive interactions between adjacent carboxyl groups.

To gain insight into the relative importance of anion–anion and cation–anion interactions in determining the crystal structures of these compounds, symmetry-constrained molecular mechanics energy minimizations of the structures were carried out. The Dreiding 2.2.1, Universal 1.02 and/or Compass force fields as implemented in *Cerius*² (Molecular Simulations Inc., 1998) were used where parameters were available. Energy minimizations were carried out with the lattice parameters fixed at the experimental values and as refinable parameters. Quantifying the ‘packing forces’ turns out to be difficult, even today. Such molecular mechanics calculations are limited by the parameterizations of the force fields and quantum calculations on such systems are very large.

In all cases, the dominant contribution to the crystal energy is electrostatic attractions. The van der Waals repulsion energy in dilithium terephthalate is relatively small and the cell volume does not change greatly when the lattice parameters are allowed to refine. The coordination requirements of the relatively small Li^+ cations seem to dominate, resulting in a different packing of anions.

In diammonium terephthalate, the electrostatic and hydrogen-bonding contributions to the total energy are comparable, and the van der Waals repulsion is larger than in dilithium terephthalate. Depending on the force field, the cell volume increases or decreases slightly, or remains the same. There seems to be no dominant contribution to the packing energy. The crystal energy is almost independent of the orientations of the ammonium cations; they ‘tumble’ during the minimizations. Such a flat potential energy surface undoubtedly contributes to the stacking faults which are present in

Table 11
Interatomic distances (Å) and angles (°) in the terephthalate carboxyl groups.

| Salt | C _{ring} –C _{carboxyl} | C–O | C–C–O | O–C–O | Ring–CO ₂ interplanar angle |
|---------------------------------|--|--|--|----------------------------|---|
| Li ₂ | 1.496 (3)† | 1.263 (2)† 1.272 (3)† | 119.6 (3)† 116.6 (4)† | 123.8 (10)† | 6.0 |
| (NH ₄) ₂ | 1.502‡ 1.504‡ | 1.303 (19)† 1.270 (19)† 1.244 (20)† 1.360 (18)† | 115.9 (15)† 123.4 (19)† 123.1 (15)† 113.0 (15)† | 120.7 (19)† 117.2 (21)† | 29.0 30.8 |
| Na ₂ | 1.498 (6)† 1.503 (6)† | 1.291 (7)† 1.239 (7)† 1.296 (7)† 1.249 (7)† | 120.3 (10)† 120.2 (9)† 118.6 (10)† 117.8 (9)† | 119.3 (10)† 121.4 (11)† | 24.9 21.4 |
| K ₂ | 1.517 (5) | 1.260 (5) 1.261 (3) | 116.9 (2) 118.7 (3) | 124.4 (3) | 6.6 |
| KH | 1.492 (5) | 1.227 (4) 1.294 (4) | 121.5 (4) 115.2 (4) | 123.3 (3) | 8.4 |
| NH ₄ H | 1.491 (4) | 1.235 (3) 1.294 (3) | 120.8 (2) 116.7 (2) | 122.5 (2) | 9.6 |

† Subject to soft constraints. ‡ Rigid body.

Table 12
Short axes and interplanar angles in monpositive terephthalate salts.

| Salt | Short cell axis (Å) | Interplanar angle (°) |
|---------------------------------|---------------------|-----------------------|
| Li ₂ | 5.13208 (2) | 67.8 |
| (NH ₄) ₂ | 4.0053 (5) | 52.0 |
| Na ₂ | 3.54805 (5) | 56.3 |
| K ₂ | 3.9440 (12) | 50.0 |
| KH | 3.770 (2) | 46.5 |
| (NH ₄)H | 3.7967 (9) | 45.7 |

this material. Anion–anion and cation–anion interactions seem closely balanced.

The short C···C intermolecular distances (as short as 3.14 Å), the relatively large van der Waals repulsion energy and the expansion of the cell volume on energy minimization indicate that the crystal structure of disodium terephthalate is

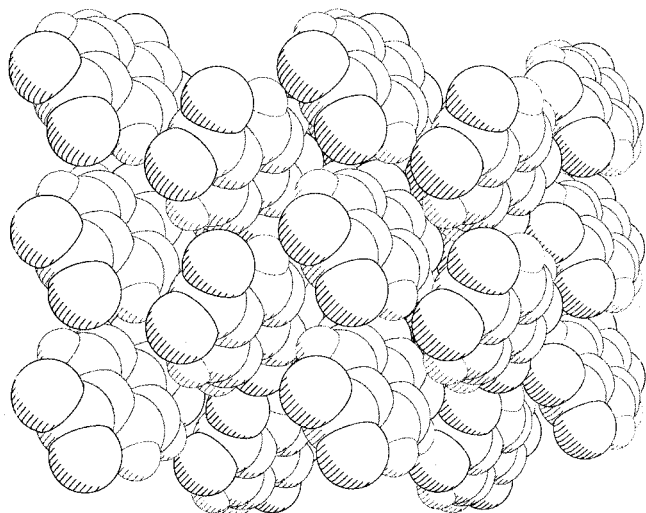


Figure 12
The γ packing of the terephthalate anions in dilithium terephthalate. The view is down the monoclinic *a* axis.

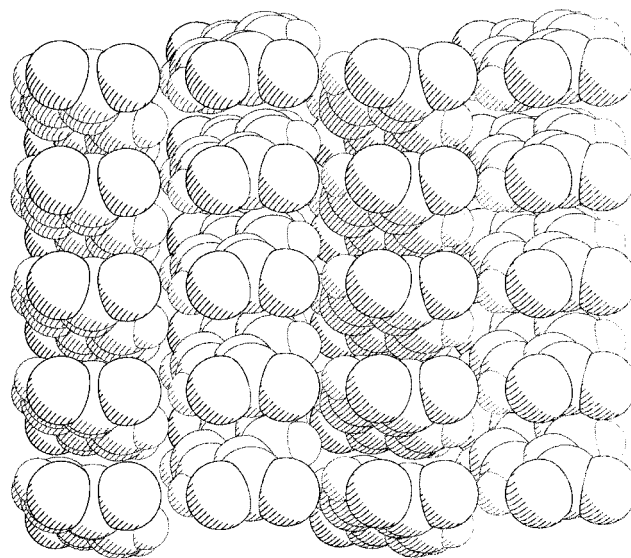


Figure 13
The β packing of the terephthalate anions in disodium terephthalate. The view is down the orthorhombic *c* axis.

dominated by cation–anion interactions, resulting in ‘crowding’ of the anions.

The cell volume of dipotassium terephthalate actually decreases slightly on energy minimization and the van der Waals repulsion energy is smaller than those in the other salts. The potassium cation seems to be a better ‘match’ to the terephthalate anion than does the sodium cation. The structures of the two acid salts turn out to be difficult to model using any of the three force fields. The hydrogen bonds certainly contribute significantly to the crystal energy. The similarity of the anion packing to that in the other structures indicates that electrostatic attractions among the carboxyl groups are important to the packing energy.

The crystal structures of several bis(ammonium) salts of terephthalic acid have been reported. They include hexamethylenediammonium terephthalate dihydrate (Moritani *et al.*, 1990; CSD Refcode JEGVIA), piperazinium terephthalate (Kashino *et al.*, 1973; CSD Refcode PIZTPH), 1,2-bis(3,4,5,6-tetrahydropyrimidin-2-yl)ethane terephthalate (Hosseini *et al.*, 1994; CSD Refcode POFREH), ethylenediammonium terephthalate (Moritani & Kashino, 1991; CSD Refcodes VIGROS and VIGRUY) and tetramethylenediammonium terephthalate (Moritani & Kashino, 1991; CSD Refcodes VIGROS and VIGRUY). Although layers are also prominent features of these structures, the layers are very different from those observed here. Each layer contains both cations and anions, with an *ABAB* packing such as that of the sodium chloride structure. These structures are not helpful in understanding the inorganic terephthalate salts reported here.

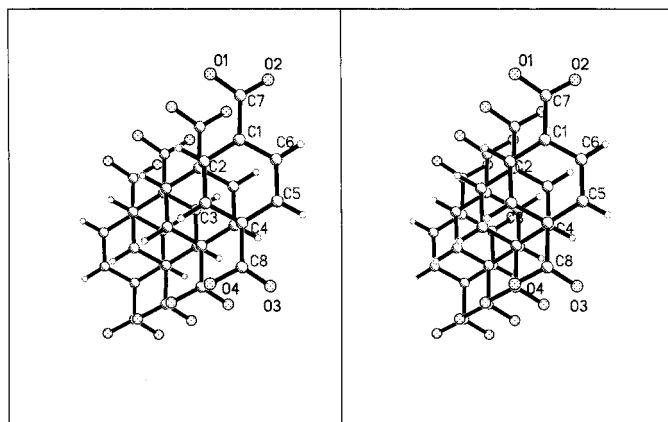


Figure 14
A stereo view of the stacking of parallel terephthalates in the β -structures, using the disodium salt as an example.

In the structure of copper(II) terephthalate trihydrate (Cueto *et al.*, 1991), one carboxyl group bridges Cu atoms to form chains, while the other is hydrogen bonded to water molecules. The two independent carboxyl groups are rotated 14 and 15° out of the ring plane. The TA packing is similar to the γ packing observed in dilithium terephthalate, but differs in detail. In the structure of calcium terephthalate trihydrate (Matsuzaki & Itaka, 1977), only one of the carboxylates is coordinated to the Ca and the other participates in hydrogen bonds. The carboxylates are rotated 5.7 and 4.0° out of the ring plane. The Ca coordination is trigonal prismatic. The parallel stacking of the terephthalates differs from those observed here, and resembles those in the polymorphs of terephthalic acid.

Many of these structures share a common motif for terephthalate packing. This β packing might be expected to persist in the structures of other terephthalate salts. Given the many possible binding modes of a carboxylate to a metal atom, we can expect a great variety of new structures for metal terephthalates, especially as the cation/anion ratio and the degree of hydration are varied. Both electrostatic interactions among the anions and the coordination requirements of the metal cations will be important in determining the crystal packing.

Thanks are given to R. Chesnut for preparing ammonium hydrogen terephthalate and his initial interest in these compounds, and P. W. Stephens for the collection of the synchrotron data for dilithium and disodium terephthalate. This work represents research carried out in part at the National Synchrotron Light Source at Brookhaven National

Laboratory, which is supported by the US Department of Energy, Division of Materials Sciences and Division of Chemical Sciences. The SUNY X3 PRT beamline at NSLS is supported by the Division of Basic Energy Sciences of the US Department of Energy (grant DE-FG02-86ER-45231).

References

- Allen, F. H. & Kennard, O. (1993). *Chem. Des. Autom. News*, **8**, 31–37.
- Barker, R. S. & Saffer, A. (1958). US Patent 2,833,816.
- Boultif, A. & Louer, D. (1991). *J. Appl. Cryst.* **24**, 987–993.
- Brese, N. E. & O'Keefe, M. (1991). *Acta Cryst.* **B47**, 192–197.
- Brzyska, W. (1971). *Ann. Univ. Mariae Curie-Sklodowska Sect. AA*, **26/27**, 105–111.
- Cobbledick, R. E. & Small, R. W. H. (1972). *Acta Cryst.* **B28**, 2924–2928.
- Cueto, S., Gramlich, V., Petter, W. & Rys, P. (1991). *Acta Cryst.* **C47**, 75–78.
- Desiraju, G. R. & Gavezzotti, A. (1989a). *Acta Cryst.* **B45**, 473–482.
- Desiraju, G. R. & Gavezzotti, A. (1989b). *J. Chem. Soc. Chem. Commun.* pp. 621–623.
- Ebara, N. & Furuyama, S. (1973). *Sci. Pap. Coll. Gen. Educ. Univ. Tokyo*, **23**, 29–33.
- Furuyama, S. & Ebara, N. (1967). *Sci. Pap. Coll. Gen. Educ. Univ. Tokyo*, **17**, 81–88.
- Gavezzotti, A. & Desiraju, G. R. (1988). *Acta Cryst.* **B44**, 427–434.
- Hosseini, M. W., Ruppert, R., Schaeffer, P., De Cian, A., Kyritsakas, N. & Fischer, J. (1994). *J. Chem. Soc. Chem. Commun.* pp. 2135–2136.
- Jeffrey, G. A. (1997). *An Introduction to Hydrogen Bonding*. Oxford University Press: New York.
- Kaduk, J. A. & Golab, J. T. (1999). *Acta Cryst.*, **B55**, 85–94.
- Kashino, S., Sasaki, M. & Haisa, M. (1973). *Bull. Chem. Soc. Jpn*, **46**, 1375–1379.
- Larson, A. C. & Von Dreele, R. B. (1998). *GSAS*. Los Alamos National Laboratory, Los Alamos, USA.
- Matsuzaki, T. & Itaka, Y. (1977). *Acta Cryst.* **B28**, 1977–1981.
- Meyer, D. H. (1971). US Patent 3,584,039.
- Miyakubo, K., Takeda, S. & Nakamura, N. (1994). *Bull. Chem. Soc. Jpn*, **67**, 2301–2303.
- Molecular Simulations Inc. (1996). *InsightIII*, Version 2.0. Molecular Simulations Inc., 9685 Scranton Road, San Diego, CA 92121, USA.
- Molecular Simulations Inc. (1997). *Cerius²*, Version 3.5. Molecular Simulations Inc., 9685 Scranton Road, San Diego, CA 92121, USA.
- Molecular Simulations Inc. (1998). *Cerius²*, Version 3.9. Molecular Simulations Inc., 9685 Scranton Road, San Diego, CA 92121, USA.
- Moritani, Y. & Kashino, S. (1991). *Acta Cryst.* **C47**, 461–463.
- Moritani, Y., Kashino, S. & Haisa, M. (1990). *Acta Cryst.* **C46**, 846–849.
- Nicolet Instrument Corporation (1988). *SHELXTL-Plus*, Release 3.4. Nicolet Instrument Corporation, Madison, Wisconsin, USA.
- Partenheimer, W. (1995). *Chem. Ind.* **62**, 307–317.
- Sheldrick, G. M. (1990). *Acta Cryst.* **A46**, 467–473.
- Sheldrick, G. M. (1997). *SHELXTL*, Version 6. Siemens Analytical X-ray Instruments Inc., Madison, Wisconsin, USA.
- Sherif, F. G. (1970). *Ind. Eng. Chem. Prod. Res. Dev.* **9**, 408–412.
- Visser, J. W. (1969). *J. Appl. Cryst.* **2**, 89–95.